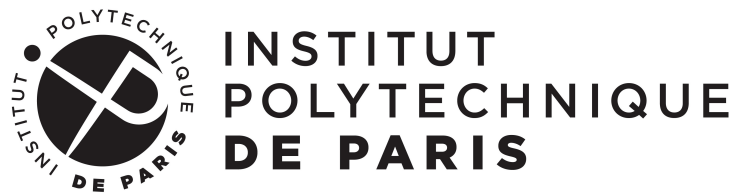

Progress report

QCD at high energy and high density: theory, links with statistical physics problems, and phenomenology

Anh-Dung LE
Supervised by: Stéphane MUNIER

September 28, 2020

Contents

1 Introduction

The high-energy regime of QCD is a unique playground for studying the field properties at high field strength (in other words, when the parton densities are large) but weak coupling, which allows for perturbative expansions as a starting point. The dynamics of hadronic matters in this regime is one of the most exciting, and challenging, problems for high energy physics, which has been being addressed in different theoretical studies. On the experimental side, various investigations toward better understandings of the low-x_{Bj} physics have been conducted in high-energy colliders in different laboratories such as HERA [1], Tevatron [2] and LHC (for example, the CMS experiment [3]). Furthermore, future electron-ion colliders (EICs) [4, 5] are expected to provide new opportunities for the study of the low-x_{Bj} dynamics in the near future.

One important theoretical question is the behavior of QCD evolution at low-x_{Bj}. Soft gluon emissions at the high-energy limit of QCD requires the resummation of the large longitudinal logarithm which, at leading logarithmic approximation (LLA), leads to an evolution equation (BFKL) [6] in the linear regime, i.e. the low-density regime in which the dynamical equations are linear. This equation predicts a rapid rise in the gluon density and, hence, the scattering amplitude when decreasing x_{Bj}, which eventually violates the Froissart-Martin unitary bound [7]. The restoration of the unitarity by including non-linear dynamics relevant at high densities is realized in various approaches proposed, for example, by Gribov, Levin and Ryskin [8], Mueller and Qiu (GLR-MQ equation) [9], by Ayalan, Gay Ducati and Levin (AGL equation) [10], or more systematically, by Jalilian-Marian, Iancu, McLerran, Weigert, Leonidov and Kovner (JIMWLK equation) [11], and Balitsky and Kovchegov (BK equation) [12]. The JIMWLK approach results in a renormalization group equation for the color glass condensate (CGC) describing the low-x_{Bj} dynamics in the regime of very high density, which is particularly difficult to investigate due to its infinite hierachy structure. In the limit of large number of colors, it reduces to the BK equation, a non-linear integro-differential equation which is practically simpler for investigations of the properties of its solution in both analytical and numerical aspects (for a throughout review, see [13]).

It was known that, the high energy QCD is similar to a reaction-diffusion problem [14], and that [15] the BK equation is in the same universality class of the Fisher-Kolmogorov-Petrovsky-Piscounov (FKPP) equation [16] which belongs to the class of reaction-diffusion equations in statistical physics. This asymptotic universality allows to solve for the asymptotic solution to the BK equation in a certain kinematic region [15], and to reproduce the geometric scaling in deep inelastic scattering [17]. Also, one can adapt the statistical approach to study fluctuations in partonic evolution [18, 19] to which the dynamics in the dilute tail of the BK front is very sensitive. Statistical physics, therefore, can provide powerful tools to attack various problems related to the QCD high-energy evolution.

In this project, we concentrate on the QCD evolution in the context of deep inelastic virtual photon-nucleus scattering. On the theoretical side, we are working on a better understanding of nonlinear evolutions in the BK framework which emerge from QCD in the high-energy regime using tools of field theory and of statistical physics. In particular, we would like to look into the structure of evolution of the virtual photon in the interaction with nucleus from a picture of parton fluctuations. This picture also provides a new approach to the diffractive dissociation, in particular the rapidity gap distribution, in DIS, which is another interest of the thesis. Furthermore, as the understanding of the tip of branching-diffusion processes is important from both statistical physics and QCD points of view, we develop new techniques to examine this specific region. Finally, we perform a numerical analysis on the diffractive dissociation in DIS with the scope to product qualitative predictions to EIC projects.

The report is organised as follows. We will start by introducing in brief the theoretical frameworks for the study in Section 2. Section 3 is dedicated for presenting the progress of the thesis for which we summarize our works which were already published or are in preparation. Finally, we draw some conclusions and prospects in the last section.

2 Theoretical frameworks

2.1 Dipole picture of deep inelastic scattering and low-x_{Bj} evolution

Deep inelastic scattering (DIS) is defined as a scattering process in which a nucleus or a nucleon is probed by a highly energetic lepton. Here we concentrate on the DIS of a electron off a nucleus. This scattering is mediated by a virtual photon exchange, which probes the nucleus's internal structure. Since the lepton current can be factorized out, the process can be viewed as the virtual photon-nucleus interaction (see Fig. 1).

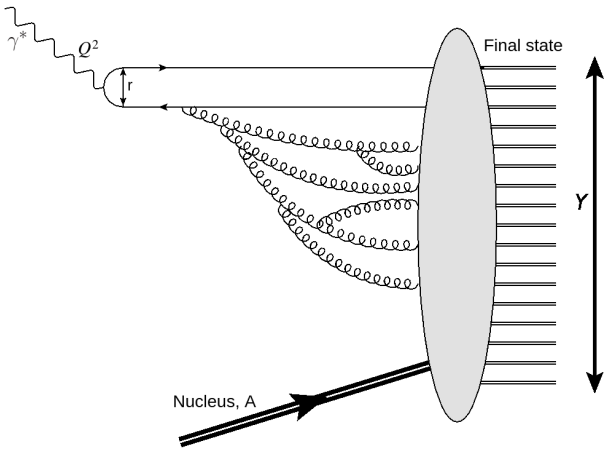

Figure 1: DIS in the dipole picture. The virtual photon interacts with the nucleus via its quark-antiquark Fock state dressed by a gluon cascade generated by soft gluon emissions.

Let us stick to the rest frame of the nucleus. At high energy, the virtual photon of virtuality Q^2 fluctuates into a color-neutral dipole consisting of a quark and an antiquark, which hereafter will be refered to as an onium, long before the interation with the nucleus. This onium evolves until the interaction time, and scatters off the nucleus as a multi-parton Fock state due to quantum fluctuations. Furthermore, since the onium has the longitudinal momentum much larger than the momentum transfered when traversing the nucleus, the size of the onium varies by a negligible amount during the interaction, and hence, the S-matrix is diagonal with respect to the transverse dipole size. This picture allows to formulate the process in the transverse coordinate space and to factorize the DIS total cross section to the dipole level as

$$\sigma_{\rm tot}^{\gamma^* A}(Q^2, Y) = \int d^2\boldsymbol{r} \int_0^1 dz \left\{ |\psi_T(\boldsymbol{r}, z, Q^2)|^2 + |\psi_L(\boldsymbol{r}, z, Q^2)|^2 \right\} \sigma_{\rm tot}^{q\bar{q}A}(\boldsymbol{r}, Y), \tag{1}$$

where we integrate over all possible transverse size vectors $\boldsymbol{r}$ of the onium and all momentum fractions z of the onium carried by the quark. The net rapidity Y of the onium-nucleus scattering is given by $Y = \ln\left(x_{0Bj}/x_{Bj}\right)$, where x_{0Bj} is the starting point of the evolution. The wave functions of the quantum fluctuation $\gamma^* \to q\bar{q}$ in the longitudinal (L) and transverse (T) polarizations are given by:

$$|\psi_L(\boldsymbol{r}, z, Q^2)|^2 = \frac{\alpha_{\rm em} N_c}{2\pi^2} 4Q^2 z^2 (1-z^2) \sum_f e_f^2 K_0^2(r a_f) \tag{2}$$

$$|\psi_T(\boldsymbol{r}, z, Q^2)|^2 = \frac{\alpha_{\rm em} N_c}{2\pi^2} \sum_f e_f^2 \left\{ a_f^2 K_1^2(r a_f) \left[z^2 + (1-z)^2 \right] + m_f^2 K_0^2(r a_f) \right\}, \tag{3}$$

where $r = |\boldsymbol{r}|$, m_f and e_f are mass and electric charge of the quark flavor f, and $a_f^2 = Q^2 z(1-z) + m_f^2$. We can write the total onium cross section in term of the onium forward scattering

amplitude $N(\boldsymbol{r}, \boldsymbol{b}, Y)$ per unit impact parameter $\boldsymbol{b}$ as

$$\sigma_{\rm tot}^{q\bar{q}A}(\boldsymbol{r}, Y) = 2\int d^2\boldsymbol{b} N(\boldsymbol{r}, \boldsymbol{b}, Y) = 2\sigma_0 N(r, Y), \tag{4}$$

where we assume the impact parameter independence of N in such a way that the $\boldsymbol{b}$-integration gives an overal dimensionful factor σ_0. With this assumption, the scattering amplitude depends only on the onium scalar size r and the net rapidity Y.

As mentioned above, the onium does not interact with the nucleus as a bare dipole, but as a multi-parton Fock state emerging from subsequent soft gluon emissions during the evolution. In the limit of large number of colors N_c, emitted gluons can be replaced by a zero-size quark-antiquark pair (color dipole), and one gluon emission from the original dipole can be seen as the one-to-two dipole branching process. The probability for the original (parent) dipole of transverse size $\boldsymbol{r}$ to split into two subsequent (daughter) dipoles of transverse sizes $\boldsymbol{r_1}$ and $\boldsymbol{r_2} = \boldsymbol{r} - \boldsymbol{r_1}$ calculated in the leading logarithmic approximation is given by the following kernel [20]:

$$K^{LO}(\boldsymbol{r}, \boldsymbol{r_1}, \boldsymbol{r_2}) = \frac{\bar{\alpha}_s}{2\pi}\frac{r^2}{r_1^2 r_2^2}, \tag{5}$$

wheren LO stands for "leading order", and $\bar{\alpha}_s \equiv \frac{\alpha_s N_c}{\pi}$ is the coupling of the strong interaction fixed at some value. This is known as Mueller's color dipole model [20]. The splitting will be iterated in subsequent daughters to the end of the evolution and, hence, the evolution in rapidity is essentially the sequence of independent decays of dipoles into pairs dipoles creating a dipole cascade. This implies that the evolution of the onium scattering amplitude N is then governed, at LO, by the Balitsky-Kovchegov (BK) equation [12]:

$$\begin{aligned}\partial_Y N(r, Y) = \int d^2\boldsymbol{r_1} K^{LO}(\boldsymbol{r}, \boldsymbol{r_1}, \boldsymbol{r_2}) \big[N(r_1, Y) + N(r_2, Y) - N(r, Y) \\ - N(r_1, Y)N(r_2, Y)\big].\end{aligned} \tag{6}$$

The initial condition is some function representing the scattering amplitude at a certain starting rapidity. We can start at $Y = 0$ with the McLerran-Venogupalan model [21],

$$N_{\rm MV}(r, Y = 0) = 1 - \exp\left\{-\frac{r^2 Q_{s0}^2}{4}\ln\left(e + \frac{4}{r^2\Lambda_{QCD}^2}\right)\right\}, \tag{7}$$

where Λ_{QCD} is the QCD scale, and Q_{s0} is the so-called saturation momentum characterizing the nucleus at zero rapidity. One can see that, $N_{MV} \to 0$ as $r \to 0$ (color transparency), and $N_{MV} \to 1$ as $r \to +\infty$ (black-disk limit). In addition, there is a sharp transition between those two limits at $r \simeq 2/Q_{s0}$. When the evolution is turned on, the transition occurs at some Y-dependent size $r = 2/Q_s(Y)$, where $Q_s(Y)$ is the saturation momentum at rapidity Y, defined, for example, from the following requirement:

$$N(r = 2/Q_s, Y) = \frac{1}{2}. \tag{8}$$

It was known [15, 17, 22–26] that the nuclear saturation scale Q_s from the LO kernel grows fast, which remarkably limits the application of the LO BK equation on the phenomenological studies. The inclusion of the running coupling, on the other hand, significantly slows down the evolution, making theoretical predictions more realistic for experimental data. The running coupling BK (rcBK) equation was found [27] to be in the same form as Eq. (6), with the LO kernel replaced by a running coupling kernel K^{rc}, which is not uniquely determined, since it depends on the scheme used to regularize an UV divergence. Different prescriptions for K^{rc} can be found in [27, 28].

2.2 Diffractive dissociation in DIS (DDIS)

One of the most fascinating observations at DESY HERA for the deep inelastic virtual photon-proton scattering is the single diffractive dissociation [29] in which the proton is kept intact, leaving a rapidity gap, namely an angular sector around the direction of the scattered proton which can be characterised by the rapidity variable Y_0, with no particles produced. This diffraction is analogous to what happens in optics: if light is incident on a black disk, the shadow of the disk is not perfectly black, but dressed by a pattern due to diffraction. In the same way, the counterpart of absorption of a quantum particle by a disk (e.g., a large nucleus) is diffraction, which is characterised by the elastic scattering. Therefore it is naturally to expect the same thing to happen for the scattering of a virtual photon off a large nucleus from the quantum mechanical point of view.

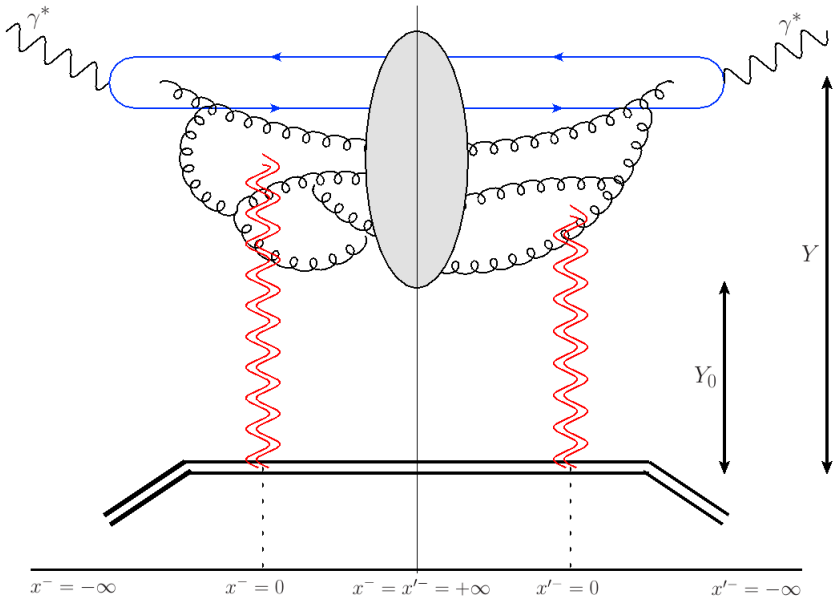

Figure 2: Diffractive dissociation in DIS with a minimal rapidity gap Y_0. The vertical continuous line represents the final state at $x^- = x'^- = +\infty$. The amplitude is to the left and the conjugate amplitude is to the right of this line. Interactions at $x^- = 0$ ($x'^- = 0$) with the nucleus are mediated by color-neutral objects represented by double wavy lines.

In fact it was realized that the dipole picture of DIS led to phenomenological successes [30] in describing the DESY HERA data on total and diffractive DIS. A crucial point of this model is that, the understanding of the photon scattering is translated into the understanding of the onium scattering. For the latter, an exact non-linear evolution equation to describe the diffractive dissociation was derived from QCD in the limit of large N_c [31], which reads

$$\begin{aligned}\partial_Y N^D_{Y_0}(r,Y) = \int d^2\boldsymbol{r_1} K^{LO}(\boldsymbol{r},\boldsymbol{r_1},\boldsymbol{r_2}) \big[& N^D_{Y_0}(r_1,Y) + N^D_{Y_0}(r_2,Y) - N^D_{Y_0}(r,Y) \\ & -2N(r_1,Y)N^D_{Y_0}(r_2,Y) - 2N(r_2,Y)N^D_{Y_0}(r_1,Y) \\ & +N^D_{Y_0}(r_1,Y)N^D_{Y_0}(r_2,Y) + 2N(r_1,Y)N(r_2,Y)\big] ,\end{aligned} \tag{9}$$

where $N^D_{Y_0}(r,Y)$ is the diffractive cross section with a minimal rapidity gap Y_0 at a net rapidity Y of an onium of size r off a nucleus at fixed impact parameter. Since the scattering with the rapidity gap equal to the net rapidity is elastic, the equality

$$N^D_{Y_0}(r, Y = Y_0) = N^2(r, Y_0) \tag{10}$$

is used as the initial condition of Eq. (9). As for the case of the BK equation (6), Eq. (9) is written in the leading order. The running coupling version can be obtained [32] by replacing the

LO kernel K^{LO} by the running coupling kernel K^{rc} which is used to solve the rcBK equation for the initial condition (10).

Eq. (9) together with its running coupling versions form an elegant formalism for the onium-nucleus diffractive dissociation. However, due to their complex structure, no analytical solutions are known and, therefore, other approaches are required. On the other side, they can be solved numerically, providing a powerful tool for numerical and phenomenological studies (see, for example, [33]).

2.3 QCD evolution at low-x_{Bj} as a stochastic process

In the limit of large N_c, the QCD evolution of the onium is a dipole branching-diffusion process in the space of (logarithmic) dipole size with evolution variable Y, which turns out to belong to the class of one-dimensional branching Brownian motions (BBMs). It was also conjectured [15] that the LO BK equation (6) governing the parton evolution at fixed impact parameter is in the universality class of the Fisher- Kolmogorov-Petrovsky-Piscounov (FKPP) equation [16], a partial parabolic differential equation which characterizes some properties of the realizations of BBMs (for a review, see [34]). This universality allows the BK equation to admit a traveling wave solution, namely a front translated at some velocity while its shape is essentially unchanged, at asymptotic large rapidities. In other words, the asymptotic amplitude N does not depend on $\ln\frac{1}{r}$ and Y separately, but depends on the so-called scaling variable $\ln\frac{1}{rQ_s(Y)}$. This traveling wave behavior is corresponding to the geometric scaling [35, 36] manifested in DIS. In particular, the traveling wave solution with the finite-Y correction reads

$$N(r,Y) = c_N \left(r^2 Q_s^2(Y)\right)^{\gamma_0} \ln\left(\frac{1}{r^2 Q_s^2(Y)}\right) \exp\left[-\frac{\ln^2\left(\frac{1}{r^2 Q_s^2(Y)}\right)}{2\chi''(\gamma_0)\bar{\alpha}Y}\right], \tag{11}$$

where c_N is some constant, and the saturation momentum scale at large rapidities is given by

$$Q_s^2(Y) = Q_{s0}^2 \exp\left[\chi'(\gamma_0)\bar{\alpha}Y - \frac{3}{2\gamma_0}\ln\bar{\alpha}Y + \text{const} + O\left(\frac{1}{\sqrt{Y}}\right)\right], \tag{12}$$

where $\chi(\gamma) = 2\psi(1) - \psi(1-\gamma) - \psi(\gamma)$ is the characteristic function of linearized BK kernel ($\psi(\gamma)$ is the digamma function). The critical value γ_0 is determined from the condition $\chi'(\gamma_0) = \chi(\gamma_0)/\gamma_0$, whose numerical value is $\gamma_0 \approx 0.63$. The solution (11) is valid for $Y \gg 1$, and for r in the so-called (geometric) scaling region:

$$1 < \ln\frac{1}{r^2 Q_s^2(Y)} < \sqrt{\chi''(\gamma_0)\bar{\alpha}Y}. \tag{13}$$

For the sake of convenience, and for the link to the branching-diffusion problems, we will use the following variables:

$$\begin{aligned} y &\equiv \bar{\alpha}Y; \qquad x \equiv \ln\frac{1}{r^2 Q_{s0}^2}; \\ \bar{X}_y &\equiv \ln\frac{Q_s^2(Y)}{Q_{s0}^2}. \end{aligned} \tag{14}$$

In term of these new variables, the amplitude N can be rewritten as

$$N(x,y) = c_N (x - \bar{X}_y) e^{-\gamma_0(x-\bar{X}_y) - \frac{(x-\bar{X}_y)^2}{2\chi''(\gamma_0)y}}, \tag{15}$$

and the scaling window (13) is translated into $1 < x - \bar{X}_y < \sqrt{\chi''(\gamma_0)y}$. The variable x, which is the logarithmic size of the onium, is now refered to as position. The parameter $\bar{X}_y$ is called the "position" of the traveling wave solution (front), which is nothing but the logarithm of the saturation scale. Its expression is

$$\bar{X}_y = \chi'(\gamma_0)y - \frac{3}{2\gamma_0}\ln y + \text{const} + O\left(\frac{1}{\sqrt{y}}\right). \tag{16}$$

Let us now look at the partonic configuration of the onium in the interaction with a nucleus in the scaling window at a total rapidity y. As the onium lying outside the nuclear saturation boundary, the interaction is triggered by rare fluctuations [18, 19, 37] in the onium's Fock state occurring in the course of the evolution. One can picture the rare fluctuations as follows. In the reference frame where the nucleus is boosted to the rapidity y_1, the onium will evolve to the rapidity $\tilde{y}_1 \equiv y - y_1$. The evolution of a single onium at position x from zero rapidity to some rapidity $\tilde{y}_1$ by branching and diffusion processes develops a stochastic tree with the boundary (tip) $X_{\tilde{y}_1}$, which is a random variable defined to be the smallest position (largest size) of dipole in the realization. At low rapidities when the number of dipoles is small, the tree is subject to fluctuations that shift its typical shape, namely the mean value of the boundary $\langle X_{\tilde{y}_1} \rangle$, by a certain amount. They are called "front fluctuations". On the other hand, fluctuations can also occur near the tip at large rapidities $\tilde{y}_1 \gg 1$ when the number of dipoles is dense, which are refered to as "tip fluctuations". This model of rare fluctuations can provide us some insights into the onium-nucleus scattering process, and hence, will be employed in our investigations.

3 Thesis progress

At this stage, we have published our work [38] which is to establish a Monte Carlo (MC) event generator to generate particles in the tip of branching random walks (BRWs). In addition, we discussed the analogy between the diffraction and the genealogy of partonic evolution in [39, 40]. For the time being, our works on the onium-nucleus scattering configuration and genealogy, and on the phenomenology of diffraction in the virtual photon-nucleus scattering are in preparation, which would be available soon. For the remaining time of the Ph.D. study, we are expecting to finish the study of the tip region using the established MC algorithm, and to figure out the full asymptotics of the diffraction. Let us discuss in some detail these projects.

3.1 Onium-nucleus scattering in different frames

We consider the scattering of a single onium at position x in the deep scaling region $1 \ll (x - \bar{X}_y) \ll \sqrt{\chi''(\gamma_0) y}$ off a nucleus at a net rapidity y. As mentioned in the previous section, the interaction in this set up is induced by rare fluctuations. We shall examine how rare fluctuations manifest in three different scenarios: *i*) the nucleus is kept at rest and all evolution is in the onium, *ii*) the nucleus is slightly boosted to a rapidity y_0 such that $1 \ll y_0 \ll (x - \bar{X}_y)^2$, and *iii*) the nucleus is highly boosted to a rapidity y_0 such that $y_0 \gg (x - \bar{X}_y)^2$.

In the frame where the nucleus is boosted to a rapidity y_0, the onium will evolve to the rapidity $\tilde{y}_0 \equiv y - y_0$. Each dipole at position x' in the state of the onium interacts independently with the nucleus with the amplitude given by the solution to the BK equation:

$$\bar{N}(y_0, x') = C_N (x' - \bar{X}_{y_0}) e^{-\gamma_0 (x' - \bar{X}_{y_0})} \exp\left(-\frac{(x' - \bar{X}_{y_0})^2}{2\chi''(\gamma_0) y_0} \right) \Theta(x' - \bar{X}_{y_0}), \tag{17}$$

for $y_0 \gg 1$. For the nucleus at rest, $y_0 = 0$, $N(0, x')$ is given by the McLerran-Venogupalan profile, which can be safely replaced by a Heaviside step function.

Suppose that there is a fluctuation in the onium Fock's state after the evolution rapidity $\tilde{y}_1 < \tilde{y}_0$ which sends a single dipole to a distance $\delta > 0$ from the mean-field tip $\langle X_{\tilde{y}_1} \rangle$. The distribution of this fluctuation size also solves the BK equations:

$$p(\delta, \tilde{y}_1) = C \delta e^{-\gamma_0 \delta} \exp\left(-\frac{\delta^2}{2\chi''(\gamma_0) \tilde{y}_1} \right). \tag{18}$$

We also assume that this fluctuation will develop a deterministic front upon further rapidity evolution (from now on, this front is refered to as the $\delta-$front) whose overlap with the nucleus,

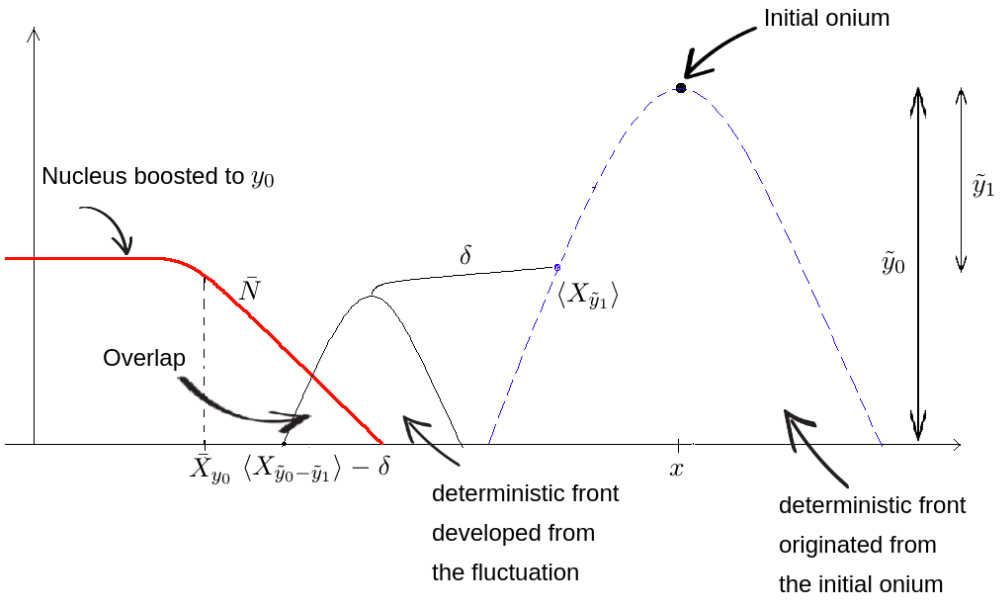

Figure 3: A schematic illustration of the configuration in the onium-nucleus scattering in the scaling window at net rapidity y and in the frame where the nucleus is boosted to the rapidity y_0. The onium at x will evolve to a front in the evolution up to rapidity $\tilde{y}_0 \equiv y - y_0$. At rapidity $\tilde{y}_1$ with respect to the onium, there is a fluctuation δ beyond the mean-field tip $\langle X_{\tilde{y}_1}\rangle$ of the main front originated from the initial onium. This fluctuation eventually develops a deterministic front during the rapidity $\tilde{y}_0 - \tilde{y}_1$ which overlaps with the nucleus profile. Each dipole at x' in the onium's Fock state is probed by the nucleus with the probability $\bar{N}(y_0, x')$ (scattering amplitude, red curve).

in the concerning kinematic region, dominatedly contributes to the scattering (see Fig. 3). The density of dipoles at position x' of this front reads

$$\bar{n}_\delta(\tilde{y}_0-\tilde{y}_1, x') = C_1 \left(x' - \langle X_{\tilde{y}_0-\tilde{y}_1}\rangle + \delta\right) e^{\gamma_0\left(x' - \langle X_{\tilde{y}_0-\tilde{y}_1}\rangle + \delta\right) - \frac{\left(x' - \langle X_{\tilde{y}_0-\tilde{y}_1}\rangle + \delta\right)^2}{2\chi''(\gamma_0)(\tilde{y}_0-\tilde{y}_1)}} \Theta\left(x' - \langle X_{\tilde{y}_0-\tilde{y}_1}\rangle + \delta\right), \tag{19}$$

where

$$\langle X_{\tilde{y}_0-\tilde{y}_1}\rangle = x - \chi'(\gamma_0)(\tilde{y}_0 - \tilde{y}_1) + \frac{3}{2\gamma_0}\ln\left(\tilde{y}_0 - \tilde{y}_1\right) + \text{const} + O\left(\frac{1}{\sqrt{\tilde{y}_0 - \tilde{y}_1}}\right). \tag{20}$$

Within this model, we can write down the onium-nucleus scattering amplitude as follows:

$$N(y, x) = \int_{y_0}^{y} dy_1 \int_0^\infty d\delta p(\delta, \tilde{y}_1)\left(1 - e^{-I(\delta, y_1)}\right), \tag{21}$$

where

$$I(\delta, y_1) = \int dx' \bar{n}_\delta(\tilde{y}_0 - \tilde{y}_1, x')\bar{N}(y_0, x') \tag{22}$$

is the overlap of the δ-front with the nucleus. We showed that the boost invariance is indeed manifested in this model: three scenarios give the same result for the scattering amplitude as in Eq. (15). However, the scattering configuration strongly depends on the choice of the frame. In the rest frame of the nucleus, since the the nucleus does not evolve to a front, we need fluctuations to send at least one dipole cross the nuclear boundary, so that it can be completely absorbed by the nucleus. The most likely picture in this case is the combination of a front fluctuation in the early stage and a tip fluctuation occuring in the very end of the onium evolution. For the second scenario in which the nucleus is slighly boosted, the fluctuation occurs at rapidity $\tilde{y}_1$ close to

$\tilde{y}_0$ such that $(\tilde{y}_0 - \tilde{y}_1) \sim y_0$, so that the fluctuation-induced front can significantly overlaps with the front of the nucleus. Finally, the scattering configuration in the case of highly-boosted nucleus is dominated by fluctuations occuring very early in the course of the evolution, namely front fluctuations.

Let us now look into the genealogy of the onium evolution. If we trace back the evolution, all dipoles probed by the nucleus should originate from a single dipole, which is refered to as the last common ancestor. In the above discussion, the last common ancestor should split between $\tilde{y}_1$ and $\tilde{y}_0$ when measured from the onium. A natural question arises: what is the distribution of the rapidity y_1 measured form the nucleus at which the last common ancestor splitted?

To quantify this problem, let us call $G(y, r; y_1)$ the joint probability distribution of y_1 and the interaction probabiliy. One can derive [39, 40] the exact equation for G in the color dipole model in the similar way to derive the BK equation for N. In the model of rare fluctuations plus the mean-field approximation, G can be computed from the following formula:

$$G(y, x; y_1) = \int_0^\infty d\delta p(\delta, \tilde{y}_1) \left\{ 1 - [1 + I(\delta, y_1)] \, e^{-I(\delta, y_1)} \right\}, \tag{23}$$

with $I(\delta, y_1)$ defined in Eq. (22). We found that the distribution is expressed as:

$$\frac{G(y, x; y_1)}{N(y, x)} = \frac{1}{\gamma_0} \frac{1}{\sqrt{2\pi\chi''(\gamma_0)}} \left(\frac{y}{y_1(y - y_1)} \right)^{3/2}, \tag{24}$$

which is identical, up to a correspondence, to the result of a similar genealogical problem on branching random walks and directed polymers [41]. Eq. (24) is valid for an asymptotically large y, and for $y_1, (y - y_1) \gg 1$. This distribution was conjectured [37, 39, 40, 42] to be related to the rapidity gap distribution in the onium-nucleus diffractive dissociation, which are going to be discussed.

3.2 Rapidity gap ditribution in DDIS

Consider the scattering of quantum particles on a disk. If the disk is almost transparent, or $S \sim 1$, elastic events are unlikely to be observed since $\sigma_{el} = (1 - S)^2 \sim 0$. If, instead, the disk is fully absorptive (black-disk), or $S \sim 0$, then $\sigma_{el} \simeq \sigma_{inel} \simeq \sigma_{tot}/2$, and the elastic scattering occurs in half of events. Furthermore, the elastic scattering is due to the particles which are diffracted in the disk's shadow. Therefore, to have diffraction, one needs to approach the black-disk limit.

Back to the onium-nucleus interaction in the scaling window, let us consider a frame in which the nucleus is boosted to a rapidity $y_0 \gg 1$, and hence, the onium will evolve to the rapidity $\tilde{y}_0 = y - y_0$ ($\tilde{y}_0 \gg 1$). The onium does not interact with the nucleus as a bare dipole, but as a highly evolved Fock state. The state of the onium at $\tilde{y}_0$ can be subject to a rare fluctuation which could create a few unusually large dipoles in the evolved onium state whose sizes are greater than the inverse nuclear saturation scale $1/Q_s(y_0)$. These dipoles interact with the nucleus with a probability of order unity. From the above discussion, the black-disk limit is realized, and the scattering with nucleus is elastic in half of events, which results in a diffractive event with a rapidity gap y_0. Meanwhile, partons loose their coherence due to independent interactions with the nucleus, so the onium is dissociated and fragmentated to the final state. As a result, we have the single diffraction. Adopting this picture of fluctuation and a statistical interpretation of the BK equation, one can deduce [37, 42] the distribution for the rapidity gap which reads

$$\frac{1}{\sigma_{tot}^{q\bar{q}A}} \frac{d\sigma_{diff}^{q\bar{q}A}}{dy_0}(y_0|y, x) = c_{diff} \left[\frac{y}{y_0(y - y_0)} \right]^{3/2}. \tag{25}$$

We see that the gap distribution (25) is similar to the ancestry distribution (24), up to an overall constant. In addition, two distributions are related to the history of the evolution at

some moderate rapidity y_0. Therefore, we expect a subtle relation between these two problems, which we are trying to figure out.

One can also employ the above formulation for the model of rare fluctuations plus mean-field approximation, together with the Good-Walker formulation of diffraction [43], to compute the rapidity gap distribution in the diffractive onium-nucleus scattering. We ended up with a formula of the same functional form as Eq. (25), and with the overall constant completely determined. However, there are still some fuzzy points of this approach that we need to clarify. Therefore, we shall leave the result of this approach to a future discussion.

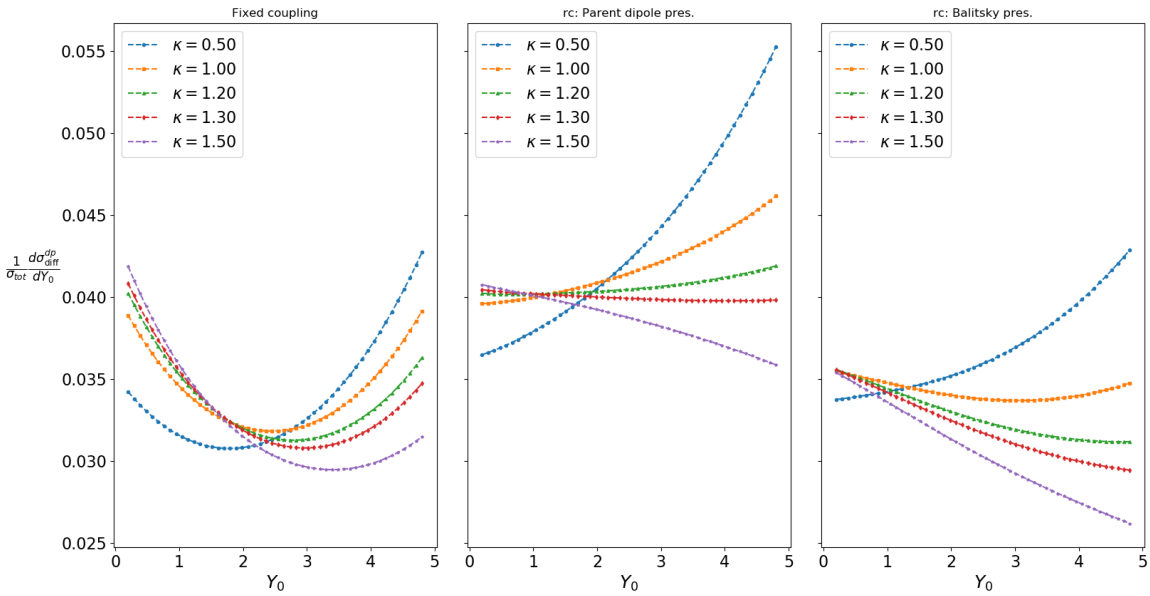

Figure 4: Rapidity gap distributions for the diffractive onium-nucleus scattering at net rapidity $Y = 5$. The first graph is for the fixed coupling, while two remaining ones are for the running coupling but with two different prescriptions. Onium sizes are picked according to the condition $\ln \frac{1}{r^2 Q_s^2(Y)} = 2\kappa Y^{1/4}$.

An analytical understanding of the asymptotic distribution of rapidity gap is important as it is the first step toward a formulation of the rapidity gap distribution for moderate rapidities, which are useful for phenomenological investigations. However, since we are still far from this goal, a numerical analysis is necessary to figure out some properties of the distribution for practical values of net rapidity. This is available with the dipole model of DIS and the nonlinear BK and KL evolution equations in both fixed-coupling and running-coupling scenarios. As it is still in progress, we just show here (Fig. 4) some preliminary numerical results in the case of onium-nucleus scattering for both fixed and running coupling scenarios.

3.3 Tip of BRWs: a Monte Carlo investigation

As discussed above, the scattering of an onium off a nucleus in the case of the onium size much smaller than the nuclear saturation scale is sensitive to the tip of the dipole branching-diffusion front, i.e. the region close to the rightmost (or leftmost) particle. In many other applications of BBMs and BRWs, it is also important to understand the tip region. Therefore, it is particularly important to examine this region in both analytical (for example, [44, 45]) and numerical aspects. For the latter, we establish a Monte Carlo (MC) algorithm to generate the tip of branching randoms walks evolved to large times [38].

3.3.1 The algorithm

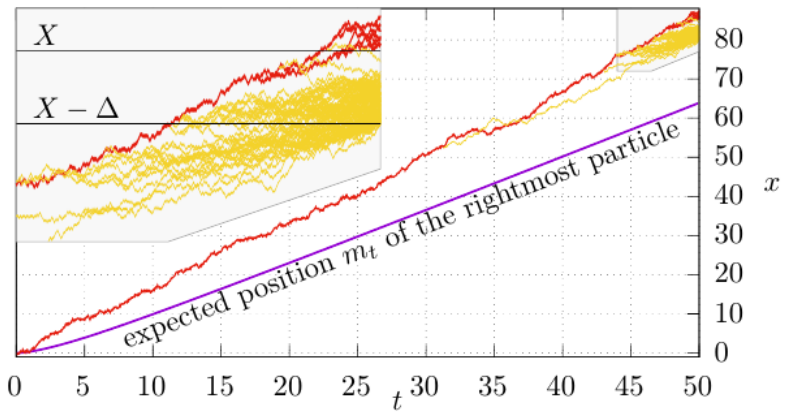

Figure 5: A realization of constrained BRW up to $T = 50$, with $X = 85.1$ and $\Delta = 5$. This figure is adapted from [38].

Since the direct MC simulation for BRWs and BBMs is impractical due to the exponential increase of particle number with the simulation time, we proposed an effective algorithm [38] which allows to generate an one-dimensional BRW to a large time T, keeping only the particles that arrive within an interval $[X - \Delta, +\infty)$ with the condition that there is at least one particle to the right of X (for an illustration, see Fig. 5). The algorithm can be summarized as follows.

We consider a BRW on an one-dimensional lattice with step size δx forward in time with step δt. This BRW is originated from a particle at $x = 0$ at the initial time $t = 0$. For each evolution step from t to $t + \delta t$, a particle at position x in the system can evolve in following three manners:

(i) Jumping from x to $x + \delta x$, with probability p_r,

(ii) Jumping from x to $x - \delta x$, with probability p_l,

(iii) Branching into two particles without moving, with probability r,

with $p_r + p_l + r = 1$. Let R_t be the position of the rightmost particle at time t, and introduce $u(x,t) = \mathcal{P}(R_t \geq x)$, the probalility that R_t lie to the right of position x. Then u solves the following equation:

$$u(x, t + \delta t) = p_r u(x - \delta x, t) + p_l u(x + \delta x, t) + r u(x,t)\left[2 - u(x,t)\right], \tag{26}$$

with the initial condition $u(x, 0) = 1 - \delta(x)$.

The first goal of the algorithm is to generate realizations of the trajectories of all red particles which are defined as those whose rightmost offspring lies in $[X, +\infty)$ after the time horizon T, given that the initial particle is also red. This can be done by employing, instead of p_r, p_l and r, following probabilities:

i. Probability that a particle at (x,t) jumps right given that it is red:

$$\mathcal{P}\left(\text{right}|\text{red}\right) = p_r \frac{U(x + \delta x, t + \delta t)}{U(x,t)}. \tag{27}$$

ii. Probability that a particle at (x,t) jumps left given that it is red:

$$\mathcal{P}\left(\text{left}|\text{red}\right) = p_l \frac{U(x - \delta x, t + \delta t)}{U(x,t)}. \tag{28}$$

iii. Probability that a particle at (x,t) branches into two red particles given that it is red:

$$\mathcal{P}\left(\begin{array}{c}\text{red}\\ \text{red}\end{array}\middle|\text{red}\right) = r\frac{U^2(x,t+\delta t)}{U(x,t)}. \tag{29}$$

iv. Probability that a particle at (x,t) branches into one red and one non-red given that it is red:

$$\mathcal{P}\left(\begin{array}{c}\text{red}\\ \text{non}-\text{red}\end{array}\middle|\text{red}\right) = r\frac{2U(x,t+\delta t)[1-U(x,t+\delta t)]}{U(x,t)}. \tag{30}$$

In these formulae, U(x,t) is the probability that a given particle at (x,t) is red, and by definition, related to $u(x,t)$ as: $U(x,t) = u(X-x, T-t)$.

The above procedure can be extended to the second goal of the algorithm, that is to follow paths of all particles whose rightmost offspring is in the interval $[X-\Delta, X)$ for some $\Delta > 0$ after the time T, which are refered as the green particle. In addition, for completeness, we define blue particles to be those whose rightmost offspring is in the range $(-\infty, X-\Delta)$. Since non-red = green + blue, we can replace the probability Eq. (30) by two following probability:

$$\mathcal{P}\left(\begin{array}{c}\text{red}\\ \text{green}\end{array}\middle|\text{red}\right) = r\frac{2U(x,t+\delta t)V_\Delta(x,t+\delta t)}{U(x,t)} \tag{31}$$

and

$$\mathcal{P}\left(\begin{array}{c}\text{red}\\ \text{blue}\end{array}\middle|\text{red}\right) = r\frac{2U(x,t+\delta t)[1-U(x+\Delta,t+\delta t)]}{U(x,t)}, \tag{32}$$

where $V_\Delta(x,t) = U(x+\Delta,t) - U(x,t)$, which is the probability for a particle at (x,t) to be green. For a particle which is conditioned to be green, the probability that it moves or branches into two greens are given, correspondingly, by Eqs. (27) to (29), with U replaced by V_Δ. Finally, the branching to one green and one blue from an green is given by the following probability:

$$\mathcal{P}\left(\begin{array}{c}\text{green}\\ \text{blue}\end{array}\middle|\text{green}\right) = r\frac{2V_\Delta(x,t+\delta t)[1-U(x+\Delta,t+\delta t)]}{V_\Delta(x,t)}. \tag{33}$$

While the above algorithm allows to follow all particles ending in the interval $[X-\Delta, +\infty)$ at time T conditioned that there is at least one particle to the right of X, one can readily modify it to the case in which the rightmost particle is fixed at X precisely. In addition, we can take the continuous limit to see how, in principle, can generate the tip for the BBM, which gives a starting point for further analytical investigations of the frontier region.

The algorithm allows to study observables of the tip for which no other method is available to date (for example, the distribution of particles at distance a to the left of the rightmost particle). Furthermore, it can be employed to study other problems, such as the genealogical structure of particles in the tip, which is closely related to the genealogical problem of the QCD evolution.

3.3.2 Particle density in the tip

Prior to the establishment of the above algorithm, we already published a preprint [46] in which we introduced an algorithm to generate realizations of BRWs in which there is at least one particle to the right of some predefined position X_{min} at the final time T at which one analyzes the set of particles. Using the implementation of that algorithm, we were able to generate ensembles of realizations in which the position X of the rightmost particle is effectively unconstrained (by setting X_{min} to a value smaller than the mean position of the rightmost particle $\langle R_T \rangle$) or constrained (with X_{min} chosen in the scaling region). With those ensembles, we were able to derive some numerical results on the probabilities $p_n(\Delta x)$ of the particle numbers

n in an interval of variable size Δx to the left of the rightmost particle, and on the mean and typical numbers of particles in this tip region.

However, that algorithm itself contains a flaw, which was pointed out by Éric Brunet and then, brought to our attention. Fixing that flaw not only produces the above correct algorithm to generate the tip of BRWs but also gives a theoretical description of the conditioned BBM which may be useful to give a mathematical description of the tip. Furthermore, we have checked that, in the case of $T = 1000$ and $X_{min} = 1400$, the numbers obtained for the observables calculated with the new, correct, code are indistinguishable from the old one. So, we expect that some conclusions in the preprint [46] are still valid.

At present, we are collecting and analysing the data. The results are expected to be released in the upcoming time.

4 Conclusions and prospects

In conclusion, the aim of this thesis is to gain some theoretical understandings on different problems relevant to the QCD evolution at low-x_{Bj}. And to date, we have advanced the study in numerous aspects. In the first place, we developed the model of rare fluctuations in the wave function of the onium and used it to examine the onium's configuration in the scattering off a nucleus. We showed that the shape of fluctuations dominantly contributing to the interaction strongly depends on the scenario of boosting the nucleus. In addition, the model provides an elegant appoach to the study of the genealogical structure of the partons in the tip of the branching-diffusion front of the onium which are probed by the nucleus. Notably, we obtained, from the model, the distribution of the branching time of their last common ancestor, which well agrees with the result for a problem of the same class in statistical physics. Furthermore, we developed an effective Monte Carlo algorithm to generate realizations of the tip in BRWs evolved to large times, which enables the study of various observables of the tip as well as the history of particles in the tip of the evolution.

In the meantime, there are several works which are in preparation. The model of rare fluctuations also enables to study the rapidity gap distribution in the diffractive onium-nucleus scattering for which we are trying to clean up all the points. Besides, we are also looking for some behaviors of the diffractive DIS from a numerical calculation, which could be a starting point for the connection to the EIC experiments. For the statistical physics aspect, a numerical investigation of some characteristics of the tip of BRWs by employing the established algorithm is being conducted.

The study opens up many possible developments. On the statistical aspect, one can examine the genealogical problem from a more rigorous point of view of statistical physics. Furthermore, we intend to develop a theoretical formulation of branching-diffusion processes which allows to provide a method to calculate observables of the tip. This approach is important since an analytical, and systematic, understanding of the frontier and relevant structures is always a big request.

There are also many things to do, and to expect, from the QCD point of view. One probable consideration is to inherit the mechanism to generate the tip of BRWs to construct a Monte Carlo algorithm for the QCD dipole evolution which can produce ensembles for the configurations of nuclear scattering. In addition, since the current analysis on the diffraction is in the asymptotic region, it would be worth to work out sub-asymptotic corrections, and hence, to be more phenomenologically relevant. Also, we would like to extend our work to address the diffraction in proton-nucleus collision, which is another dilute-dense scattering comparing to the onium-nucleus scattering considered in this study.

References

[1] A. M. Cooper-Sarkar, R. C. E. Devenish, and A. De Roeck. Structure functions of the nucleon and their interpretation. *Int. J. Mod. Phys. A*, 13:3385, 1998.
H. Abramowicz and A. C. Caldwell. HERA collider physics. *Rev. Mod. Phys.*, 71:1275, 1999.
A. M. Cooper-Sarkar. Low x physics at HERA. In *30th International Symposium on Multiparticle Dynamics*, page 73, 2001.

[2] C. Pajares. RHIC physics. *Acta Phys. Polon. B*, 30:2263, 1999.

[3] A. Grebenyuk. CMS forward and small-x QCD physics results. *Nuclear and Particle Physics Proceedings*, 270-272:13, 2016. 18th Montpellier International Conference on Quantum Chromodynamics (QCD 15).
R. Gupta. Recent CMS results on soft and small-x QCD physics. *EPJ Web Conf.*, 206:06006, 2019.

[4] Daniel Boer et al. Gluons and the quark sea at high energies: Distributions, polarization, tomography, 2011. Report No. SLAC-R-995, INT-PUB-11-034, BNL-96164-2011, JLAB-THY-11-1373. arXiv:1108.1713.

[5] A. Accardi et al. Electron Ion Collider: The Next QCD Frontier: Understanding the glue that binds us all. *Eur. Phys. J. A*, 52:268, 2016.

[6] L. N. Lipatov. Reggeization of the Vector Meson and the Vacuum Singularity in Nonabelian Gauge Theories. *Sov. J. Nucl. Phys.*, 23:338, 1976.
E. A. Kuraev, L. N. Lipatov, and V. S. Fadin. The Pomeranchuk Singularity in Nonabelian Gauge Theories. *Sov. Phys. JETP*, 45:199, 1977.
I. I. Balitsky and L. N. Lipatov. The Pomeranchuk Singularity in Quantum Chromodynamics. *Sov. J. Nucl. Phys.*, 28:822, 1978.

[7] M. Froissart. Asymptotic behavior and subtractions in the Mandelstam representation. *Phys. Rev.*, 123:1053, 1961.
A. Martin. *Scattering Theory: Unitarity, Analyticity and Crossing*, volume 3 of *Lecture notes in Physics*. Springer-Verlag, 1969.

[8] L. V. Gribov, E. M. Levin, and M. G. Ryskin. Semihard Processes in QCD. *Phys. Rept.*, 100:1, 1983.

[9] A. H. Mueller and J. W. Qiu. Gluon Recombination and Shadowing at Small Values of x. *Nucl. Phys. B*, 268:427, 1986.

[10] A. L. Ayala, M. B. Gay Ducati, and E. M. Levin. Unitarity boundary for deep inelastic structure functions. *Phys. Lett. B*, 388(1):188, 1996.
A. L. Ayala, M. B. Gay Ducati, and E. M. Levin. QCD evolution of the gluon density in a nucleus. *Nucl. Phys. B*, 493:305, 1997.
A. L. Ayala, M. B. Gay Ducati, and E. M. Levin. Parton densities in a nucleon. *Nucl. Phys. B*, 511:355, 1998.

[11] J. Jalilian-Marian, A. Kovner, L. McLerran, and H. Weigert. Intrinsic glue distribution at very small x. *Phys. Rev. D*, 55:5414, 1997.
J. Jalilian-Marian, A. Kovner, A. Leonidov, and H. Weigert. The BFKL equation from the wilson renormalization group. *Nuclear Physics B*, 504:415, 1997.
J. Jalilian-Marian, A. Kovner, A. Leonidov, and H. Weigert. Wilson renormalization group for low x physics: Towards the high density regime. *Phys. Rev. D*, 59:014014, 1998.
J. Jalilian-Marian, A. Kovner, and H. Weigert. Wilson renormalization group for low x physics: Gluon evolution at finite parton density. *Phys. Rev. D*, 59:014015, 1998.
J. Jalilian-Marian, A. Kovner, A. Leonidov, and H. Weigert. Unitarization of gluon distribution in the doubly logarithmic regime at high density. *Phys. Rev. D*, 59:034007, 1999.
E. Iancu, A. Leonidov, and L. McLerran. Nonlinear gluon evolution in the color glass condensate: I. *Nucl. Phys. A*, 692:583, 2001.
Iancu E., A. Leonidov, and L. McLerran. The renormalization group equation for the color glass condensate. *Phys. Lett. B*, 510(1):133, 2001.
E. Iancu and L. McLerran. Saturation and universality in QCD at small x. *Phys. Lett. B*, 510:145, 2001.

[12] I. Balitsky. Operator expansion for high-energy scattering. *Nucl. Phys. B*, 463(1):99, 1996.
Y. V. Kovchegov. Small-x F_2 structure function of a nucleus including multiple pomeron exchanges. *Phys. Rev. D*, 60(3):034008, 1999.

[13] Y. V. Kovchegov and E. Levin. *Quantum chromodynamics at high energy*, volume 33 of *Camb. Monogr. Part. Phys. Nucl. Phys. Cosmol.* Cambridge University Press, 2012.

[14] E. Iancu, A. H. Mueller, and S. Munier. Universal behavior of QCD amplitudes at high energy from general tools of statistical physics. *Phys. Lett. B*, 606:342, 2005.

[15] S. Munier and R. Peschanski. Traveling wave fronts and the transition to saturation. *Phys. Rev. D*, 69(3):034008, 2004.

[16] R. A. Fisher. The wave of advance of advantageous genes. *Ann. Eugen.*, 7(4):355, 1937.
A. Kolmogorov, I. Petrovsky, and N. Piscounov. Study of the diffusion equation with growth of the quantity of matter and its application to a biology problem. *Moscow Univ. Bull. Math.*, A1:1, 1937.

[17] S. Munier and R. Peschanski. Universality and tree structure of high-energy QCD. *Phys. Rev. D*, 70(7):077503, 2004.

[18] A. H. Mueller and S. Munier. Phenomenological picture of fluctuations in branching random walks. *Phys. Rev. E*, 90:042143, 2014.

[19] A. H. Mueller and S. Munier. On parton number fluctuations at various stages of the rapidity evolution. *Phys. Lett. B*, 737:303 – 310, 2014.

[20] A. H. Mueller. Soft gluons in the infinite-momentum wave function and the BFKL pomeron. *Nucl. Phys. B*, 415(2):373, 1994.
A. H. Mueller and B. Patel. Single and double BFKL pomeron exchange and a dipole picture of high energy hard processes. *Nucl. Phys. B*, 425(3):471, 1994.
A. H. Mueller. Unitarity and the BFKL pomeron. *Nucl. Phys. B*, 437(1):107, 1995.

[21] L. D. McLerran and R. Venugopalan. Computing quark and gluon distribution functions for very large nuclei. *Phys. Rev. D*, 49(5):2233, 1994.
L. D. McLerran and R. Venugopalan. Gluon distribution functions for very large nuclei at small transverse momentum. *Phys. Rev. D*, 49(7):3352, 1994.

[22] E. Iancu, K. Itakura, and L. D. McLerran. Geometric scaling above the saturation scale. *Nucl. Phys. A*, 708(3):327, 2002.

[23] A. H. Mueller and D. N. Triantafyllopoulos. The energy dependence of the saturation momentum. *Nucl. Phys. B*, 640(1):331, 2002.

[24] N. Armesto and M. A. Braun. Parton densities and dipole cross-sections at small x in large nuclei. *Eur. Phys. J. C*, 20(3):517, 2001.

[25] M. A. Braun. Pomeron fan diagrams with an infrared cutoff and running coupling. *Phys. Lett. B*, 576(1):115, 2003.

[26] J. L. Albacete, N. Armesto, J. G. Milhano, C. A. Salgado, and U. A. Wiedemann. Numerical analysis of the Balitsky-Kovchegov equation with running coupling: Dependence of the saturation scale on nuclear size and rapidity. *Phys. Rev. D*, 71(1):014003, 2005.

[27] I. Balitsky. Quark contribution to the small-x evolution of color dipole. *Phys. Rev. D*, 75(1):014001, 2007.
Y. V. Kovchegov and H. Weigert. Triumvirate of running couplings in small-x evolution. *Nucl. Phys. A*, 784(1):188, 2007.

[28] J. L. Albacete and Y. V. Kovchegov. Solving the high energy evolution equation including running coupling corrections. *Phys. Rev. D*, 75(12):125021, 2007.

[29] H1 collaboration, T. Ahmed, et al. First measurement of the deep–inelastic structure of proton diffraction. *Phys. Lett. B*, 348(3):681, 1995.
ZEUS collaboration, M. Derrick, et al. Measurement of the diffractive structure function in deep inelastic scattering at HERA. *Z. Phys. C*, 68(4):569, 1995.

[30] K. Golec-Biernat and M. Wüsthoff. Saturation effects in deep inelastic scattering at low Q^2 and its implications on diffraction. *Phys. Rev. D*, 59(1):014017, 1998.
K. Golec-Biernat and M. Wüsthoff. Saturation in diffractive deep inelastic scattering. *Phys. Rev. D*, 60(11):114023, 1999.

[31] Y. V. Kovchegov and E. Levin. Diffractive dissociation including multiple pomeron exchanges in high parton density QCD. *Nucl. Phys. B*, 577(1):221, 2000.

[32] Y. V. Kovchegov. Running coupling corrections to non-linear evolution for diffractive dissociation. *Phys. Lett. B*, 710(1):192, 2012.
Y. V. Kovchegov. Running coupling evolution for diffractive dissociation and the NLO odderon intercept. *AIP Conference Proceedings*, 1523(1):335, 2013.

[33] E. Levin and M. Lublinsky. Non-linear evolution and high energy diffractive production. *Phys. Lett. B*, 521(3):233, 2001.
E. Levin and M. Lublinsky. Diffractive dissociation and saturation scale from non-linear evolution in high energy DIS. *Eur. Phys. J. C*, 22(4):647, 2002.
E. Levin and M. Lublinsky. Diffractive dissociation from nonlinear evolution in DIS on nuclei. *Nucl. Phys. A*, 712(1):95, 2002.

[34] S. Munier. Statistical physics in QCD evolution towards high energies. *Sci. China Phys. Mech. Astron.*, 58(8):81001, 2015.

[35] S. Munier and R. Peschanski. Geometric scaling as traveling waves. *Phys. Rev. Lett.*, 91(23):232001, 2003.

[36] A. M. Stato, K. Golec-Biernat, and J. Kwiecinski. Geometric scaling for the total $\gamma^* - p$ cross section in the low x region. *Phys. Rev. Lett.*, 86:596, 2001.

[37] A. H. Mueller and S. Munier. Rapidity gap distribution in diffractive deep-inelastic scattering and parton genealogy. *Phys. Rev. D*, 98:034021, 2018.

[38] É. Brunet, A. D. Le, A. H. Mueller, and S. Munier. How to generate the tip of branching random walks evolved to large times. *EPL (Europhysics Letters)*, 131(4):40002, 2020.

[39] D. Le Anh and S. Munier. Rapidity gaps and ancestry. *Acta Phys. Polon. Supp.*, 12:825, 2019.

[40] D. Le Anh. Diffractive dissociation in onium-nucleus scattering from a partonic picture.

In *18th Conference on Elastic and Diffractive Scattering (EDS Blois)*, 2019.

[41] B. Derrida and P. Mottishaw. On the genealogy of branching random walks and of directed polymers. *EPL (Europhysics Letters)*, 115:40005, 2016.

[42] A. H. Mueller and S. Munier. Diffractive electron-nucleus scattering and ancestry in branching random walks. *Phys. Rev. Lett.*, 121:082001, 2018.

[43] M. L. Good and W. D. Walker. Diffraction dissociation of beam particles. *Phys. Rev.*, 120:1857, 1960.

[44] E. Brunet and B. Derrida. A branching random walk seen from the tip. *J. Stat. Phys.*, 143:420, 2011.
E. Aïdékon, J. Berestycki, E. Brunet, and Z. Shi. Branching brownian motion seen from its tip. *Probab. Theory Relat. Fields*, 157:405, 2013.
O. Hallatschek. The noisy edge of traveling waves. *Proceedings of the National Academy of Sciences*, 108:1783, 2011.

[45] A. H. Mueller and S. Munier. Particle-number distribution in large fluctuations at the tip of branching random walks. *Phys. Rev. E*, 102:022104, 2020.

[46] A. D. Le, A. H. Mueller, and S. Munier. Monte Carlo study of the tip region of branching random walks evolved to large times. 2020. arXiv:0707.3168.